International Journal of Applied Electromagnetics and Mechanics 51 (2016) 235–248
DOI 10.3233/JAE-150093
IOS Press

A high-efficiency, self-powered nonlinear interface circuit for bi-stable rotating piezoelectric vibration energy harvesting with nonlinear magnetic force

Congcong Cheng[a], Zhongsheng Chen[a,b,*], Yeping Xiong[b], Hongwu Shi[a] and Yongmin Yang[a]
[a]*Science and Technology on Integrated Logistics Support Laboratory, National University of Defense Technology, Changsha, Hunan, China*
[b]*Faculty of Engineering and the Environment, University of Southampton, Boldrewood Campus, Southampton, UK*

Abstract. Parallel synchronized switch harvesting on inductor (P-SSHI) circuits have been proved to enhance piezoelectric vibration energy harvesting (PVEH), but the maximum conversion efficiency is obtained only when the voltage across the storage capacitor (VSC) equates to the optimal value. For bi-stable rotating PVEH with nonlinear magnetic force in engineering applications, however, the VSC will change greatly when powering real electric loads, thus it is impossible to maintain high conversion efficiency. In order to solve this problem, this paper presents an improved P-SSHI circuit with controllable optimal voltage (COV-PSSHI) by using a voltage control strategy between the storage capacitor and the electric load. The innovation is to control and maintain the VSC close to the optimal value. Firstly, the COV-PSSHI circuit is proposed and its theoretic model is built in detail. Then its average harvested power (AHP) is theoretically derived and AHP of the COV-PSSHI circuit is proved to be more than that of a classical P-SSHI circuit. In the end, experiments are performed to validate the performance of the COV-PSSHI circuit. It can be seen that the COV-PSSHI circuit can increase the AHP by factor 1.25 compared with classical P-SSHI circuits, which is enough to intermittently power the wireless sensor node. Also power consumption of the voltage control circuit has few effects on the COV-PSSHI circuit. In particular, it needs to optimize the envelop capacitor, the parallel inductor and two threshold voltages of the voltage controller in order to implement the COV-PSSHI circuit well in practice.

Keywords: Nonlinear rotating energy harvesting, bi-stable piezoelectric harvester, P-SSHI circuit, COV-PSSHI circuit

1. Introduction

Nowadays, wireless sensor networks (WSNs) are widely used in military and industrial fields due to the advantages of wireless signal transmission, low cost and easy distribution, etc. While wireless sensor nodes are always placed in highly dangerous or unreachable areas, it is necessary to provide autonomous and long-life power sources for WSNs. Therefore, the battery is not a proper solution because it has

*Corresponding author: Zhongsheng Chen, Science and Technology on Integrated Logistics Support Laboratory, National University of Defense Technology, Changsha, Hunan 410073, China. Tel.: +86 731 84574322; Fax: +86 731 84573395; E-mail: chenzhongsheng@nudt.edu.cn.

limited useful life and needs to be replaced regularly. Nowadays, vibration energy harvesting has become a research hot-spot [1–3]. In particular, piezoelectric vibration energy harvesting (PVEH) is widely studied for designing self-powered wireless sensors [4,5]. However, vibrations in some applications often need to be suppressed due to their harms to mechanical structures. In this case, the output power of a PVEH device should be much low. Fortunately, there are continuous rotating motions in many applications. Thus it is promising to harvest energy from rotating motions to overcome the problem. In the authors' previous work [6], a nonlinear rotating energy harvester by employing nonlinear magnetic force has been studied and the results demonstrated that bi-stable rotating energy harvesters are suitable for broadband rotating motions.

As we all know that the output of a bi-stable rotating piezoelectric harvester is yet a small AC voltage, so an interface circuit is needed to realize AC-DC conversion and power storage for wireless sensors. Standard energy harvesting (SEH) interface circuit composed of a full bridge rectifier has the advantage of simple structure, but its efficiency is very low. The reason is that intrinsic capacitive reactance of piezoelectric patch is often very large and varies with exciting frequencies, so that it is very difficult for SEH circuit to achieve optimal impedance matching [7,8]. Although an impedance matching circuit can be designed optimally, it cannot be adaptive to the variations of ambient vibrations, such as broadband rotating motions. In order to overcome these drawbacks, synchronized switch harvesting on inductor (SSHI) circuits have been studied and proved to increase the harvested power by several times than that of a SEH circuit under the same inputs, including parallel SSHI (P-SSHI) and series SSHI (S-SSHI) circuits [9,10]. Subsequently, SSHI circuits have been improved in many ways [11–14]. Up to now, several classes of switching strategies have been proposed, such as switching driven by external logic circuits [15], mechanical switching [16] and switching through velocity control [17]. However, these switching strategies either need external power sources or cause the electric circuit very complex, so they are not useful in many practical applications. In order to reduce the power consumption of control circuits, Lallart [18] first proposed an electronic switch circuit to make a P-SSHI circuit fully self-powered. Later, Liang et al. [19] proposed a modified self-powered P-SSHI circuit based on Lallart's circuit. Qiu et al. [20] proposed a simple source-less trigger circuit to control the synchronized switch and then designed two interface circuits of PVEH. Also, Ramadass and Chandrakasan [21] presented a bias-flip rectifier and the power extraction capability was testified to be improved by greater than 4X.

Despite of the superiority of P-SSHI circuits, but the most disadvantage is that the maximum power can be harvested only when the voltage across the storage capacitor (VSC) equates the optimal value. While in engineering applications a P-SSHI circuit always needs to be connected to a real electric load, instead of a purely resistive load [18–20], such as a wireless sensor. Then the storage capacitor will be charged or discharged periodically for the wireless sensor, so that the VSC varies and shifts continuously from the optimal value during working. In this case, it is impossible to maintain the maximum power output in most time and the conversion efficiency of the P-SSHI circuit is not the same high as expected. Therefore, it is much necessary to improve existed P-SSHI circuits from the viewpoint of engineering applications.

As for broadband rotating motions, in this paper a novel P-SSHI circuit with controllable optimal voltage (COV-PSSHI) is proposed for bi-stable rotating PVEH with nonlinear magnetic force. The goal of the COV-PSSHI circuit is to advance the previous self-powered P-SSHI circuits by using a voltage control strategy between the storage capacitor and the electric load. The voltage control circuit mainly consists of a voltage controller and a DC-DC converter. The voltage controller is powered by the storage capacitor and makes itself self-powered. The most advantage of the COV-PSSHI circuit is to control the VSC nearby the optimal value, so that high harvesting efficiency can be achieved and maintained. The

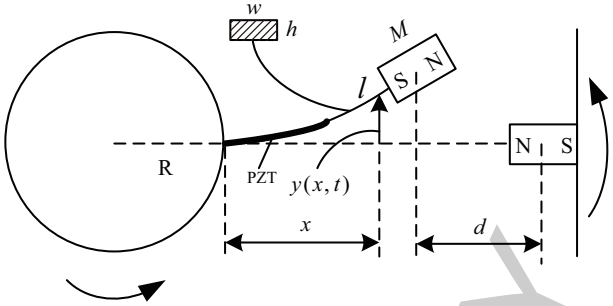

Fig. 1. Schematic diagram of a bi-stable rotating piezoelectric energy harvester.

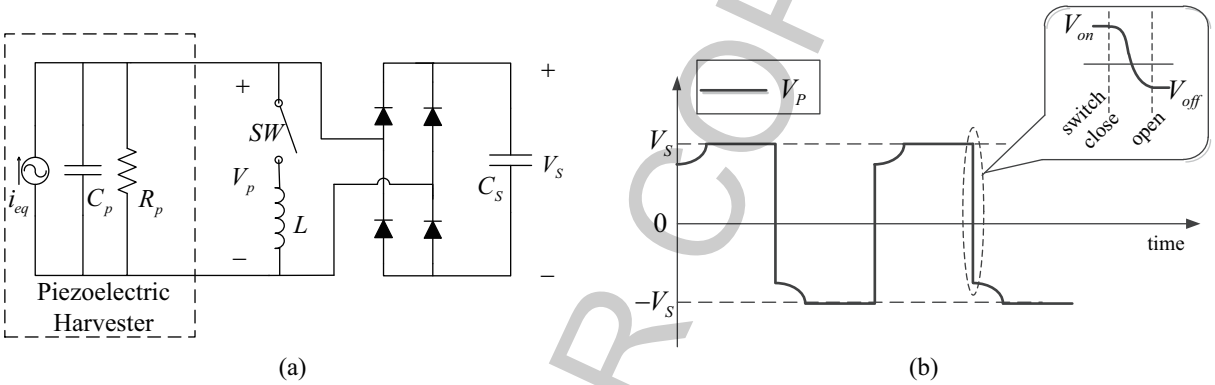

Fig. 2. (a) Schematic diagram of a P-SSHI circuit. (b) The waveform of piezoelectric voltage in the P-SSHI circuit.

innovation of this paper is to carry out voltage adaptation between a P-SSHI circuit and a real electronic load, which is less studied in previous works. The left outline of this paper is summarized as follows: In Section 2, basic principle of a P-SSHI circuit is introduced and its problem is addressed. Then a novel COV-PSSHI circuit is proposed and its theoretic model is built in Section 3. Also its average harvested power is derived. Simulations and experiments are performed in Section 4 to validate theoretical results and compare the proposed circuit with classical P-SSHI circuits. In the end, conclusions are discussed in Section 5.

2. Basic principle of P-SSHI circuits for bi-stable rotating piezoelectric energy harvesters

As stated in Ref. [6], a nonlinear rotating piezoelectric energy harvester is sketched in Fig. 1, which is composed of a piezoelectric cantilever beam and a pair of permanent magnets. When the distance between two magnets is appropriate, it will lead to a bi-stable rotating harvester. In order to match the bi-stable rotating harvester, a P-SSHI circuit should be used, instead of a SEH circuit.

The equivalent circuit of a bi-stable rotating piezoelectric harvester with a P-SSHI circuit can be modeled as Fig. 2(a), where a switching circuit is placed between the piezoelectric harvester and the rectifier. The switch is only turned on at the maximum or minimum value of the displacement. During its work cycles, the storage capacitor is charged when the absolute value of V_P is greater than the VSC (V_S). Once the displacement reaches the extreme value, the switch is turned on to form an $L - C_p$

oscillating loop. Its period is much smaller than that of exciting vibrations, so the voltage inversion can be assumed to finish instantaneously. At this time, the voltage V_p will be inversed and put in phase with velocity. Then the energy stored in the clamped capacitor C_p is extracted by the $L - C_p$ resonant circuit. After the inversion, V_p increases inversely up to $-V_S$ and the storage capacitor is charged again until next extreme value of the displacement comes. Then this voltage inversion process will repeat periodically. Ideally, if the voltage inversion on C_P is perfect, V_p should change between $+V_S$ and $-V_S$. However, the quality factor Q of the $L - C_p$ loop is finite, so that the inversion process is not ideal and the inversed voltage is always lower than $|V_S|$. The classical waveform of V_p in the P-SSHI circuit is shown in Fig. 2(b). It can be seen that the $L - C_p$ resonant circuit increases the magnitude of V_p. Hence, more energy can be extracted from the bi-stable rotating harvester.

According to Ref. [22], the harvested power of a P-SSHI circuit during one work cycle is represented as Eq. (1).

$$P = 2f_0 C_p \left(2V_{oc} - V_S(1 - e^{-\pi/2Q})\right) V_S \tag{1}$$

where, Q denotes the quality factor of the $L - C_p$ oscillating loop, f_0 is the excitation frequency and V_{oc} is the open-circuit voltage across the electrodes. We can see that the harvested power depends strongly on V_S. Furthermore, the optimal value of V_S for the maximum power can be obtained as Eq. (2) and the maximum power can be obtained as Eq. (3).

$$V_{S(opt)} = \frac{V_{oc}}{(1 - e^{-\pi/2Q})} \tag{2}$$

$$P_{\max} = \frac{\omega C_p}{\pi} \frac{V_{oc}^2}{(1 - e^{-\pi/2Q})} \tag{3}$$

According to Eqs (1)–(3), the maximum harvested power can be obtained only when $V_S = V_{S(opt)}$. In engineering applications, however, the energy stored in the storage capacitor C_s will be extracted to power electric loads, such as wireless sensors, so that a discharging process often occur to make V_S decrease dramatically. On the other hand, V_S will increase again when the storage capacitor is charged. The result is that the VSC is very difficult to be fixed at the optimal value, so that the maximum power output cannot be kept in most time. Thus it is very necessary to maintain V_S in an appropriate range nearby the optimal value $V_{S(opt)}$ to achieve high conversion efficiency.

3. Theoretical model and analysis of a COV-PSSHI circuit

In order to overcome the drawback of a typical P-SSHI circuit as mentioned before, a novel P-SSHI circuit with controllable optimal voltage (COV-PSSHI) is sketched in Fig. 3 by adding a self-powered voltage control circuit. The voltage control circuit is composed of two parts: One is a voltage controller which monitors the VSC C_s and determines the time of charging or discharging. The other is a low power consumption DC-DC converter which provides a DC voltage for the electric load.

Characteristics of the voltage controller can be represented by a hysteresis window which includes two threshold voltages: the upper threshold denotes the termination of charging the storage capacitor and the low threshold denotes the termination of discharging the storage capacitor. In this case, the waveform of V_S is shown in Fig. 4. Furthermore, if the optimal voltage $V_{S(opt)}$ lies between the two thresholds, the harvested power of a COV-PSSHI circuit will be kept close to the maximum value.

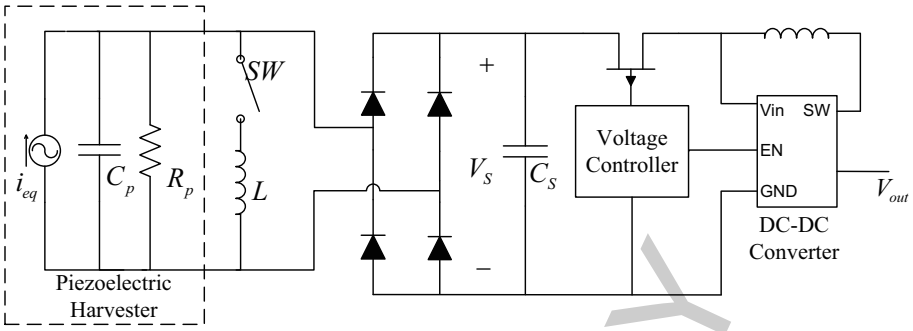

Fig. 3. Schematic diagram of the proposed COV-PSSHI circuit.

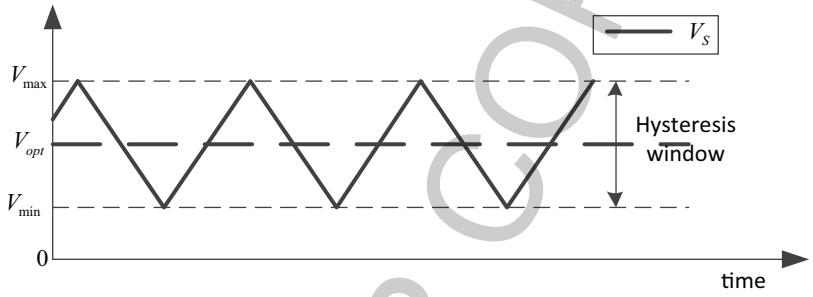

Fig. 4. Schematic diagram of controllable V_S.

Thus the conversion efficiency should be much higher than of a classical P-SSHI circuit. It must be emphasized that the excitation source always fluctuates under broadband rotating motions, so that $V_{S(opt)}$ will also vary among a range. Thus the hysteresis window should be selected depending on practical requirements. When the hysteresis window width is too small or large, the optimal voltage will be far from the hysteresis window so that the efficiency decreases dramatically. In this paper, the hysteresis window is determined based on measured open-circuit voltage of the bi-stable rotating harvester.

Furthermore, an electronic switch is adopted in Fig. 3 to make the COV-PSSHI circuit totally self-powered [23,24], which is composed of three parts: an envelope detector formed by C_1, R_1, D_1, a comparator formed by a PNP transistor T_1, and a switch formed by a NPN transistor T_2. Then the whole COV-PSSHI circuit is shown in Fig. 5 and its working mechanism can be described as follows. Firstly, when the displacement of the rotating piezoelectric harvester increases until the maximum value, the envelope detector will charge C_1 continuously. At this time, T_1 remains blocked as the voltage of its emitter is less than that of its base, so that T_2 is also blocked. Once the displacement shifts from the maximum value, the piezoelectric voltage V_P will fall below the voltage across C_1. Then T_1 is conducted and C_1 begins to be discharged through T_1, causing T_2 to conduct. Due to the symmetrical topology of the switch circuit, the switching process for the minimum displacement is the same. Secondly, when V_S is charged to the upper threshold, the voltage controller enables the DC-DC converter. Then electric energy stored in C_s is conveyed to the output capacitor C_{out}. This procedure will continue until the voltage of C_{out} reaches a pre-selected value. Then the successively harvested electric energy will continue to be accumulated in C_s. Once electric energy in C_{out} is consumed by the electric load, electric energy stored in C_s will be conveyed to C_{out} again and V_S will decrease. Once V_S falls to the low threshold, the discharging process will stop. In the end, V_S will always be kept between the two thresholds.

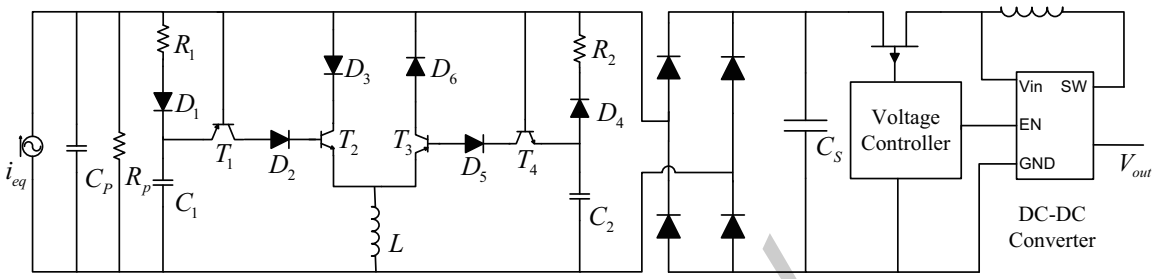

Fig. 5. Schematic diagram of the COV-PSSHI circuit with a self-powered electronic switch.

In order to analyze the performance of the COV-PSSHI circuit, a mathematical model of the harvested power needs to be built. Actually, environmental vibrations are irregular, instead of simply sinusoidal. Under this case, it is always difficult to derive the model, in particular under stochastic vibrations. For the sake of simplicity, a sinusoidal excitation source similar to many previous works [18,19] is utilized and then rotating frequency sweeping can be used to explore its broadband characteristics. That is to say, the equivalent electric current of the rotating piezoelectric harvester can be represented as

$$i_{eq} = I_0 \sin \omega t \tag{4}$$

where, I_0 is the amplitude and ω is the excitation frequency. Then we will have,

$$V_{oc} = 2I_0/\omega C_p \tag{5}$$

where V_{oc} is the amplitude of open-circuit voltage across the electrodes.

Next, we will have the following formula based on the Kirchhoff's law when the switch is turned on.

$$L_1\ddot{q} + R\dot{q} + \frac{q}{C_p} = 0 \tag{6}$$

where, q denotes the clamped charge generated by the bi-stable rotating harvester and two initial conditions before inversion are given as Eqs (7) and (8).

$$q\left(0_+\right) = q_0 = C_p V_b \tag{7}$$

$$\dot{q}\left(0_+\right) = 0 \tag{8}$$

where V_b denotes the piezoelectric voltage across the electrodes before inversion.

By solving Eq. (6), the analytical solution of q can be represented as Eq. (9).

$$q(t) = \frac{\omega_0 q_0}{\omega_1} e^{-\delta t} \sin\left(\omega_1 t + \varphi\right) \tag{9}$$

Then the piezoelectric voltage $V_p(t)$ can be obtained as Eq. (10).

$$V_p(t) = \frac{q(t)}{C_p} = \frac{\omega_0 V_b}{\omega_1} e^{-\delta t} \sin\left(\omega_1 t + \varphi\right) \tag{10}$$

And the conducting current $i(t)$ can be obtained as Eq. (11).

$$i(t) = -\frac{\omega_0^2 C_p V_b}{\omega_1} e^{-\delta t} \sin\left(\omega_1 t\right) \tag{11}$$

where,

$$\delta = \frac{r}{2L},\ \ \omega_0 = \frac{1}{\sqrt{LC_0}},\ \ \omega_1 = \sqrt{\omega_0^2 - \delta^2},\ \ \sin\varphi = \frac{\omega_1}{\omega_0},\ \ \cos\varphi = \frac{\delta}{\omega_0},\ \ Q = \frac{\omega_1}{2\delta} \tag{12}$$

At the half vibration cycle, namely $t_{off} = \pi/\omega_1$, the switch is turned off and the inversed piezoelectric voltage can be calculated as Eq. (13).

$$V_p\left(t_{off}\right) = -V_b e^{-\frac{\pi\delta}{\omega_1}} = -V_b e^{-\frac{\pi}{2Q}} \tag{13}$$

Taking the voltage drop across the diode V_D into account, the piezoelectric voltage before inversion V_b can be written as Eq. (14).

$$V_b = V_S + 2V_D \tag{14}$$

Thus, the harvested energy and power during half vibration cycle can be obtained as Eqs (15) and (16), respectively.

$$E = 2C_p V_S[V_{oc} - V_D(1 - e^{-\pi/2Q})] - C_p V_S^2(1 - e^{-\pi/2Q}) \tag{15}$$

$$P = \frac{2E}{T} = 4f_0 C_p V_S\left[V_{oc} - V_D + V_D e^{-\pi/2Q}\right] - 2f_0 C_p V_S^2\left(1 - e^{-\pi/2Q}\right) \tag{16}$$

Based on Eq. (16), the optimal voltage $V_{S(opt)}$ of the maximum harvested power can be calculated as Eq. (17).

$$V_{S(opt)} = \frac{V_{oc}}{\left(1 - e^{-\pi/2Q}\right)} - V_D \tag{17}$$

Furthermore, by substituting $V_{S(opt)}$ into Eq. (16), the maximum power output $P_{\max}$ can be calculated as Eq. (18).

$$P_{\max} = \frac{2V_{oc}^2 f_0 C_p}{\left(1 - e^{-\pi/2Q}\right)} - 2V_D f_0 C_p \tag{18}$$

It can be seen from Eq. (18) that the maximum harvested power is a function of the piezoelectric open-circuit voltage V_{oc}, the VSC V_S and the quality factor Q. At the same time, it should be noted that the maximum harvested power is independent of the storage capacitor C_s. For the COV-PSSHI circuit, when V_S is charged to the upper threshold $V_{\max}$, the voltage controller will function and the DC-DC converter is enabled. Then energy stored in C_s will be conveyed to the output capacitor C_{out}, so that V_S decreases. Once V_S falls to the low threshold $V_{\min}$, the discharging process stops. In this case, the average harvested power of the COV-PSSHI circuit is as follows.

$$\begin{aligned} P_{COV\text{-}PSSHI} = \frac{\int_{V_{\min}}^{V_{\max}} PdV}{V_{\max} - V_{\min}} &= 2f_0 C_p\left(V_{oc} - V_D + V_D e^{-\pi/2Q}\right)(V_{\max} + V_{\min}) \\ &- \frac{2}{3} f_0 C_p\left(1 - e^{-\pi/2Q}\right)\left(V_{\max}^2 + V_{\min}^2 + V_{\max} V_{\min}\right) \end{aligned} \tag{19}$$

While for a classical P-SSHI circuit with only a DC-DC converter, the converter is enabled when V_S reaches the upper threshold. Then the storage capacitor begins to be discharged and the DC-DC conversion will continue until V_S drops nearly to zero. In this case, its average harvested power can be calculated as Eq. (20).

$$P_{\textit{P-SSHI}} = \frac{\int_0^{V_{\max}} PdV}{V_{\max}} = 2f_0C_p\left(V_{oc} - V_D + V_De^{-\pi/2Q}\right)V_{\max} - \frac{2}{3}f_0C_p\left(1 - e^{-\pi/2Q}\right)V_{\max}^2 \tag{20}$$

By combining Eqs (19) and (20), the ratio of $P_{\textit{COVP-SSHI}}$ and $P_{\textit{P-SSHI}}$ can be obtained as Eq. (21).

$$k = \frac{P_{\textit{COV-PSSHI}}}{P_{\textit{P-SSHI}}} = 1 + \frac{V_m - \left(1 - e^{-\pi/2Q}\right)\left(V_D + \dfrac{V_{\min} + V_{\max}}{3}\right)}{\left(V_m - V_D + V_De^{-\pi/2Q}\right)V_{\max} - \dfrac{1}{3}\left(1 - e^{-\pi/2Q}\right)V_{\max}^2}V_{\min} \tag{21}$$

Furthermore, both $V_{\max}$ and $V_{\min}$ in the COV-PSSHI circuit are always controlled near the optimal value in order to maximize the harvested power. Without loss of generality, $V_{S(opt)}$ can be set as follows

$$V_{S(opt)} = \frac{V_{\min} + V_{\max}}{2} \tag{22}$$

Then according to Eqs (17), (21) and (22), it can be proved that k is always larger than 1. Hence, it means that the average harvested power of the proposed COV-PSSHI circuit is larger than that of classical P-SSHI circuits.

In addition, we can see from Eqs (5) and (17) that if the excitation frequency varies in a specific range, the open-circuit voltage V_{oc} will vary within a range and so is the optimum voltage. Fortunately, V_S can be maintained within the above range in the proposed COV-PSSHI circuit, so that a high conversion efficiency can be kept. Thus the proposed COV-PSSHI circuit is much fit for bi-stable rotating PVEH.

4. Experimental validations of the COV-PSSHI circuit for a bi-stable rotating piezoelectric harvester

4.1. Validations of the proposed COV-PSSHI circuit

To validate the performance of the proposed COV-PSSHI circuit, an experiment system is built as shown in Fig. 6, which is composed of a vibration generator (HEV-50), a power amplifier (HEAS-50), an impedance analyzer (Agilent 4294A), a low power consumption integrated RF transceiver and a piezoelectric cantilever beam (60 × 20 × 0.2 mm) with a double-layer piezoelectric patch in series (40 mm × 20 mm × 0.2 mm).

In the experiment, the proposed COV-PSSHI circuit is compared with a classical P-SSHI circuit by the following way: a) The same vibration excitation is used for two circuits. b) The same output capacitor (C_{out}) is used as the loads of two circuits. c) The DC/DC converter is included in the proposed COV-PSSHI circuit, while not included in the classical P-SSHI circuit. d) When the output capacitor in each

Table 1
Simulation parameters of the COV-PSSHI circuit

C_P	R_P	f_0	R_1, R_2	V_D	C_S
62 nF	3 MΩ	38.7 Hz	200 KΩ	0.5 V	100 μF

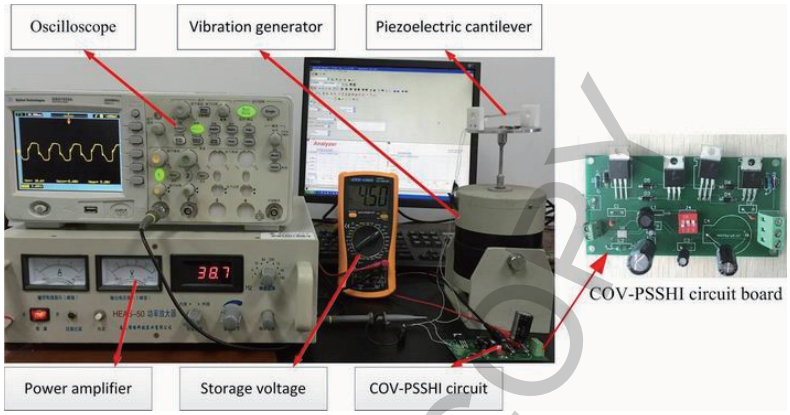

Fig. 6. Experimental set-up for testing the COV-PSSHI circuit.

circuit is charged to 3.3 V, the corresponding charging time t is recorded. Then the average harvested power is calculated by $P = \frac{1}{2}C_{out}V^2/t$. In addition, the DC/DC converter has some intrinsic power consumption. However, it is always small due to low working current and intermittent operation mode. Thus it can be neglected.

The clamped capacitor C_p and intrinsic resistor R_p of the piezoelectric patch are measures as 62 nF and 3 MΩ using the impedance analyzer, respectively. The excitation frequency is selected as 38.7 Hz close to the natural frequency of the piezoelectric beam. For given excitation frequency, the open-circuit voltage of the piezoelectric harvester can be adjustable by setting different gains of the power amplifier and then measured by the oscilloscope. In this experiment, the open-circuit voltage V_{oc} is selected as 10 V.

Firstly, key components in the electronic switch can strongly affect the switching operation according to existing work [25], especially the envelop capacitor C_1, C_2 (here $C_1 = C_2 = C_e$). Thus it is necessary to optimize them properly. In order to achieve it, the proposed COV-PSSHI circuit is modeled and simulated in the LT-SPICE software, where simulation parameters are shown in Table 1. Under the condition of $V_m = 10$ V, different values of C_e are utilized and the corresponding average harvested power stored in C_S are calculated. The relation curve is plotted in Fig. 7(a). It can be seen that there is an optimal C_e (close to 1 nF) in order to obtain the maximum harvested power. The reason is that C_e extracts energy from the piezoelectric harvester to enable the two comparators (T_1 and T_4). If C_e is too small, accumulated energy on it may not be enough to enable the two comparators, so that the electronic switch fails to work. In this case, the P-SSHI part of the COV-P-SSHI circuit will have no power output. As a result, the harvested power will decrease sharply. If C_e is too large, more energy will be stored on it so that the output power will also decrease. Similarly, the effect of the inductance L on the harvested power stored in C_S is simulated and the result is plotted in Fig. 7(b). It can be seen that the harvested power increases slowly with L. In particular, the harvested power is almost constant after L is larger than 50 mH. So we choose $C_e = 1$ nF and $L = 50$ mH in the experiment.

Secondly, it is necessary to determine two threshold voltages of the voltage controller. In order to do it, the optimal VSC of the COV-PSSHI circuit should be determined in advance. In the experiment, the

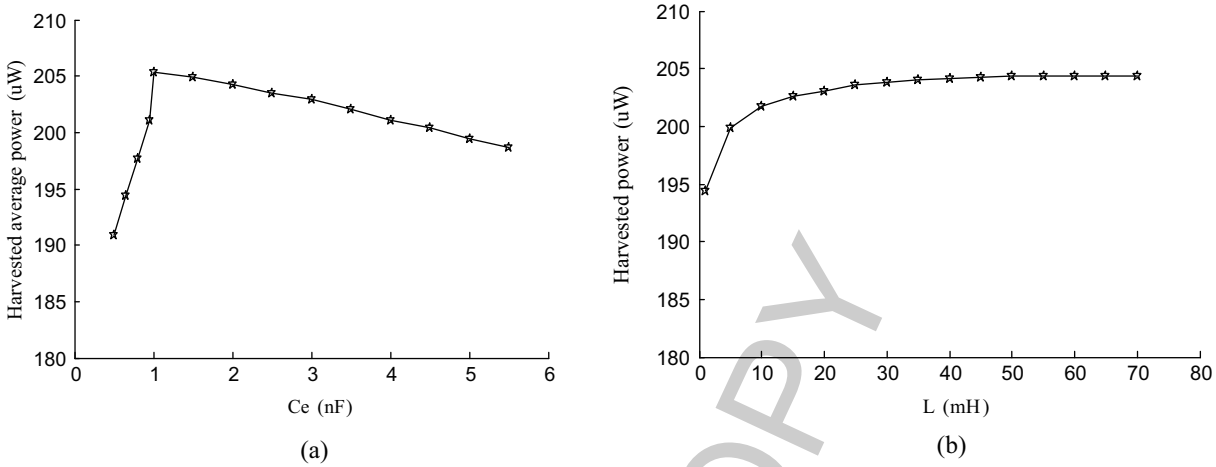

Fig. 7. The curves of the harvested power with (a) the capacitor C_e and (b) the inductance L.

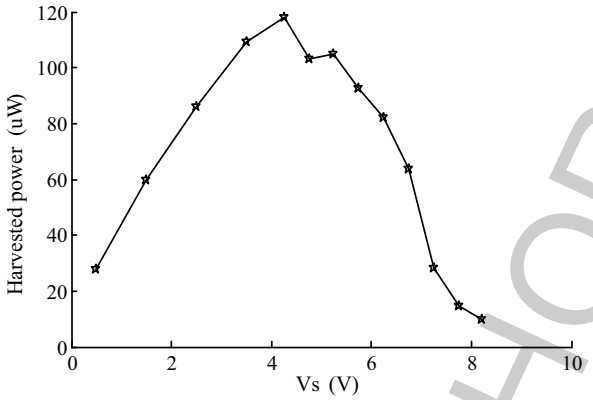

Fig. 8. The variation of the harvested average power with V_S under $V_m = 10$ V.

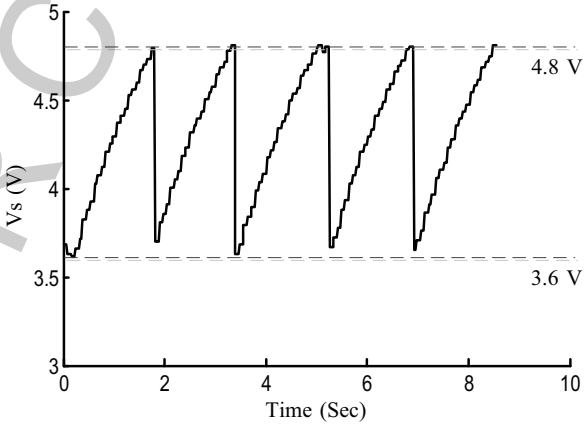

Fig. 9. The measured waveform of V_S in the COV-PSSHI circuit.

voltage control circuit in the COV-PSSHI circuit needs to be disconnected and the excitation is selected to make the open-circuit voltage across the electrodes equate to 10 V. Then the average harvested power is calculated and plotted as a function of V_S, as shown in Fig. 8. It can be seen that the optimal voltage $V_{S(opt)}$ is close to 4 V. According to Eq. (19), more power can be harvested if two threshold voltages are closer to the optimal voltage $V_{S(opt)}$. At the same time, once C_{out} has been pre-selected, the two threshold voltages have to satisfy Eq. (23), where E_{load} denotes the energy needed by the integrated RF transceiver during one working cycle.

$$\frac{C_{out}(V_{\max}^2 - V_{\min}^2)}{2} = C_{out}V_{S(opt)}(V_{\max} - V_{\min}) \geqslant E_{load} \tag{23}$$

According to Eq. (23), we can easily find that a larger output capacitor C_{out} can be used to reduce $(V_{\max} - V_{\min})$ in engineering applications. However it will lead to long charging time, even longer than the working interval of the electric load. This is not expected. Thus there should be a trade-off between

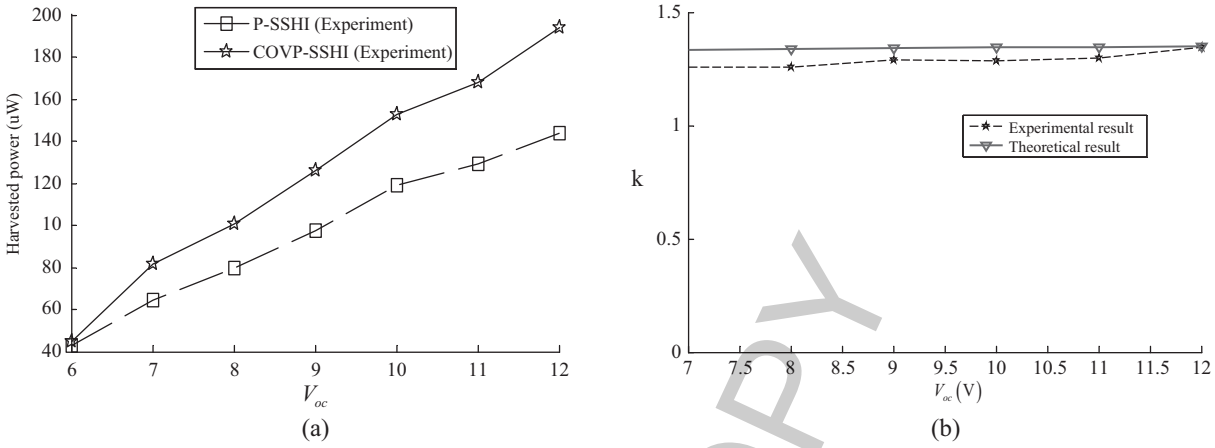

Fig. 10. (a) Harvested average powers of both circuits under different V_{oc}. (b) The variation of k with V_{oc}.

$(V_{\max} - V_{\min})$ and the output capacitor C_{out} in engineering applications (i.e., efficiency and charging time).

In this experiment, the wireless sensor node mainly consists of a low power consumption microprocessor (MSP430F2132), a temperature and humidity sensor (SHT10) and a transmitter (nRF24L01). The output voltage of the DC-DC converter is set to be 3.3 V. The operation current of the microprocessor under active mode is 450 μA. The average power consumption of the sensor under working condition is about 150 μW. The quiescent current of the transmitter is only 32 μA. While transmitting current of the transmitter is 11.3 mA and its duration time is about 288 μs. The working cycle is about 240 ms. Thus energy consumption of the sensor can be calculated as about 420 μJ during one working cycle. Based on Eq. (23), one necessary condition of the threshold window is shown in Eq. (24).

$$V_{\max} - V_{\min} \geqslant \frac{E_{load}}{C_{out} V_{S(opt)}} = 1.05 \text{ (V)} \tag{24}$$

Hence, here two voltage thresholds are set as $V_{\max} = 4.8$ V, $V_{\min} = 3.6$ V to ensure enough energy for the RF transceiver. Then the voltage control circuit in the COV-PSSHI circuit is connected and V_S is measured as Fig. 9. It can be seen that once V_S rises to 4.8 V, the voltage controller will enable the DC-DC converter. Then the storage capacitor is discharged to transfer energy to the sensor and V_S will decrease. When V_S drops to 3.6 V, the voltage controller will disable the DC-DC converter and then V_S will increase again. Thus V_S can be kept between 3.6 V and 4.8 V as expected in the experiment.

Furthermore, in order to compare the proposed COV-PSSHI circuit with a typical P-SSHI circuit [17, 18,21], the average harvested power of two circuits are measured under different open-circuit voltages V_{oc}. In the experiment, we find that the VSC cannot be charged to be larger than 4.8 V if $V_{oc} \leqslant 6$ V. In this case, the self-powered voltage control circuit cannot be enabled. Thus V_{oc} should be larger than 6 V. In order to satisfy this condition, it needs to choose a proper C_s and hysteresis window for given excitation vibrations. In addition, a low leakage capacitor should be used for C_s in practice so that the charging current is much more than the leakage current.

Then the experimental results are shown in Fig. 10(a) and two curves of k from both simulation and experiment are plotted in Fig. 10(b). One can see that the experimental results are close to the theoretical ones. Also the average harvested power of the COV-PSSHI is about 25 percent more than

Table 2
The output voltages of the COV-PSSHI circuit for the bi-stable rotating harvester

V_{out} (V)	2	3	4	5	6	7	8	9	9.6
Charging time (s)	34	59	88	114	139	168	201	229	270

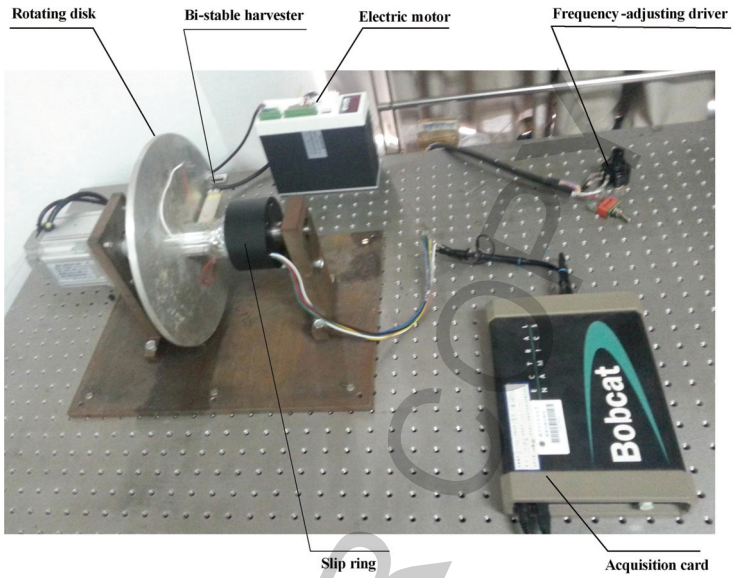

Fig. 11. Experimental set-up of a bi-stable rotating piezoelectric energy harvesting.

that of a typical P-SSHI circuit after V_m is greater than 7 V. Obviously, despite of power consumption from the self-powered voltage control circuit, the COV-PSSHI circuit can still achieve higher conversion efficiency than classical P-SSHI circuits. So we can see that power consumption of the control circuit is indeed small and has few effects on the proposed COV-PSSHI circuit.

4.2. Validations of the COV-PSSHI circuit for the bi-stable rotating piezoelectric harvester

In order to validate the COV-PSSHI circuit for the bi-stable rotating piezoelectric harvester, an experimental set-up of a bi-stable rotating piezoelectric energy harvesting is built as Fig. 11. The distance of two magnets is selected as 10 mm to construct a bi-stable rotating harvester. The proposed COV-PSSHI circuit is tested and a 4700 μF of C_{out} is used to store the harvested power.

In this experiment, the rotating speed is adjusted from 600 rpm to 1200 rpm artificially to simulate broadband rotating motions. Then the output voltage across the C_{out} is measured as Table 2. It can be seen that the output power is accumulated to about 220 mW in five minutes. Thus it is feasible to intermittently power the wireless sensor node. Also the results demonstrate that the proposed COV-PSSHI circuit is effective for bi-stable rotating PVEH.

5. Conclusions

Harvesting broadband rotating motions using bi-stable rotating piezoelectric harvesters is an effective way to power wireless sensors in engineering applications. In order to achieve it, a high-efficiency

interface circuit is needed to realize AC-DC conversion. Unfortunately, the most disadvantage of classical P-SSHI circuits is that the maximum harvested is achieved only when the VSC is equal to the optimal value. However, the VSC always varies greatly due to intermittently powering wireless sensors and broadband excitations, leading to low conversion efficiency. Therefore, this paper presented a self-powered COV-PSSHI circuit to maintain the VSC close to the optimal value. Main conclusions may include: i) Basic structure of the COV-PSSHI circuit is proposed and its mechanism is explained. ii) Theoretical model of the COV-PSSHI circuit was derived in detail. We can see that the average harvested power of the COV-PSSHI circuit can be improved greatly. iii) The innovation of the COV-PSSHI circuit is to use a self-powered voltage control circuit to keep the VSC near the optimal value. In the end, experiments were performed to validate the performance of the COV-PSSHI circuit. Thus the proposed circuit indeed provide a promising way for enhancing the conversion efficiency of bi-stable rotating PVEH. In order to implement the COV-PSSHI circuit well, two key steps should be carried out. The one is to optimize the envelop capacitor and the parallel inductor based on the open-circuit voltage of the piezoelectric harvester. The other is to optimize two threshold voltages of the voltage controller based on the power consumption of the electric load. In the end, many previous works mainly focus on how to implement the switch circuit and they still are in nature P-SSHI circuits, so the proposed idea in this paper can also be extended for them.

Acknowledgment

This work was supported by the National Natural Science foundation of China (Grant No. 51275520).

References

[1] L.G.W. Tvedt, S.N. Duy and E. Halvorsen, Nonlinear behavior of an electrostatic energy harvester under wide and narrowband excitation, *Journal of Microelectromechanical System* **19** (2010), 305–316.
[2] A. Rahimi, O. Zorlu, A. Muhtaroglu and H. Kulah, Fully self-powered electromagnetic energy harvesting system with highly efficient dual rail output, *IEEE Sensors Journal* **12** (2012), 2287–2298.
[3] J.W. Kan, J.H. Qiu, K.H. Tang, K.J. Zhu and C.H. Shao, Modeling and simulation of piezoelectric composite diaphragms for energy harvesting, *International Journal of Applied Electromagnetics and Mechanics* **30** (2009), 95–106.
[4] R. Calio, U.B. Rongala, D. Camboni, M. Milazzo, C. Stefanini, G. Petris and C.M. Oddo, Piezoelectric energy harvesting solutions, *Sensors* **14** (2014), 4755–4790.
[5] N. Kong, D.S. Ha, A. Erturk and D.J. Inman, Resistive impedance matching circuit for piezoelectric energy harvesting, *Journal of Intelligent Material Systems and Structures* **21** (2010), 1293–1302.
[6] B. Guo, Z.S. Chen, C.C. Cheng and Y.M. Yang, Characteristics of a nonlinear rotating piezoelectric energy harvester under variable rotating speeds, *International Journal of Applied Electromagnetics and Mechanics* **47** (2015) 411–423.
[7] G.K. Ottman, H.F. Hofmann and G.A. Lesieutre, Optimized piezoelectric energy harvesting circuit using step-down converter in discontinuous conduction mode, *IEEE Transactions on Power Electronics* **18** (2003), 696–703.
[8] H. Yu, J. Zhou, L. Deng and Z. Wen, A vibration-based MEMS piezoelectric energy harvester and power conditioning circuit, *Sensors* **14** (2014), 3323–3341.
[9] D. Guyomar, A. Badel, E. Lefeuvre and C. Richard, Toward energy harvesting using active materials and conversion improvement by nonlinear processing, *IEEE Transactions on Ultrasonics, Ferroelectrics, and Frequency Control* **52** (2005), 584–595.
[10] E. Lefeuvre, A. Badel, C. Richard and D. Guyomar, A comparison between several vibration-power piezoelectric generators for standalone system, *Sensors and Actuators A: Physical* **126** (2006), 405–416.
[11] J.R. Liang and W.H. Liao, On the influence of transducer internal loss in piezoelectric energy harvesting with SSHI interface, *Journal of Intelligent Material Systems and Structures* **22** (2011), 503–512.
[12] I.C. Lien, Y.C. Shu, W.J. Wu, S.M. Shiu and H.C. Lin, Revisit of series-SSHI with comparisons to other interfacing circuits in piezoelectric energy harvesting, *Smart Materials and Structures* **19** (2010), 125–134.

[13] Y.C. Shu, I.C. Lien and W.J. Wu, An improved analysis of the SSHI interface in piezoelectric energy harvesting, *Smart Materials and Structures* **16** (2007), 2253–2264.
[14] S. Lu and F. Boussaid, A highly efficient P-SSHI rectifier for piezoelectric energy harvesting, *IEEE Transactions on Industrial Electronics* **30** (2015), 5364–5369.
[15] R. Tiwari, N. Buch and E. Garcia, Energy balance for peak detection method in piezoelectric energy harvester, *Journal of Intelligent Material Systems and Structures* **25** (2014), 1024–1035.
[16] F. Giusa, A. Giuffrida, C. Trigona, B. Ando, A.R. Bulsara and S. Baglio, Random mechanical switching harvesting on inductor: A novel approach to collect and store energy from weak random vibrations with zero voltage threshold, *Sensors and Actuators A: Physical* **198** (2013), 35–45.
[17] Y.Y. Chen, Piezoelectric power transducers and its' interfacing circuitry on energy harvesting and structural damping applications, Ph.D. Thesis, National Taiwan University, Taiwan, 2013.
[18] M. Lallart and D. Guyomar, An optimized self-powered switching circuit for non-linear energy harvesting with low voltage output, *Smart Materials and Structures* **17** (2008), 3503–3511.
[19] J.R. Liang and W.H. Liao, Improved design and analysis of self-powered synchronized switch interface circuit for piezoelectric energy harvesting systems, *IEEE Transactions on In Industrial Electronics* **59** (2012), 1301–1312.
[20] J.H. Qiu, H. Jiang, H.L. Ji and K.J. Zhu, Comparison between four piezoelectric energy harvesting circuits, *Frontiers of Mechanical Engineering in China* **4** (2009), 153–159.
[21] Y.K. Ramadass and A.P. Chandrakasan, An efficient piezoelectric energy harvesting interface circuit using a bias-flip rectifier and shared inductor, *IEEE Journal of Solid-State Circuits* **45** (2010), 189–204.
[22] K.A. Singh, R. Kumar and R.J. Weber, Piezoelectric-based broadband bistable vibration energy harvester and SCE/SSHI-based high-power extraction, *Proceedings of the 11*$^{\text{th}}$ IEEE International Conference on Networking, Sensing and Control (2014), 197–202.
[23] L.Y. Zhao, L.H. Tang, H. Wu and Y.W. Yang, Synchronized charge extraction for aeroelastic energy harvesting, *Active and Passive Smart Structures and Integrated Systems* (2014), 9057.
[24] L. Zhu, R. Chen and X. Liu, Theoretical analyses of the electronic breaker switching method for nonlinear energy harvesting interfaces, *Journal of Intelligent Material Systems and Structures* **23** (2012), 441–451.
[25] M. Lallart and D. Guyomar, An optimized self-powered switching circuit for nonlinear energy harvesting with low voltage output, *Smart Materials and Structures* **17** (2008), 3503–3511.